

The analysis of an absorption rate in view of electromagnetic exposure effects exemplified by the breast cancer

Analiza współczynnika absorpcji w kontekście narażeń elektromagnetycznych na przykładzie nowotworu gruczołu piersiowego

Joanna Michałowska¹, Andrzej Wac-Włodarczyk²

¹ The State School of Higher Education, The Institute of Technical Sciences and Aviation, Chełm, Poland

² Lublin University of Technology, Institute of Electrical Engineering and Electrotechnologies, Lublin, Poland

*European Journal
of Medical Technologies*

2017; 2(15): 29-36

Copyright © 2017 by ISASDMT
All rights reserved

www.medical-technologies.eu
Published online 14.07.2017

Corresponding address:

Joanna Michałowska, The State School of Higher Education, The Institute of Technical Sciences and Aviation, 54 Pocztowa Street, 22-100 Chełm, Poland, e-mail: jmichalowska@pwsz.chelm.pl
Andrzej Wac-Włodarczyk, Lublin University of Technology, Institute of Electrical Engineering and Electrotechnologies, 38 Nadbystrzycka Street, 20-816 Lublin, Poland, e-mail: a.wac-włodarczyk@pollub.pl

Abstract

The aim of the paper is to introduce numerical analysis of a specific absorption rate in a woman body, mainly in the area of the breast. The analyzed realistic numerical breast phantoms are classified according to their radiographic density, defined by the American College of Radiology. Numerical computational electromagnetics simulations can be used as Empire XCcel software based on the finite-difference time-domain (FDTD) method. The results were compared with the current Directive (Directive 2013/35 / EU). It has been shown that the microwave tomography method is safe.

Key words:

breast cancer, SAR
(specific absorption rate), microwave tomography,
electromagnetic fields

Streszczenie

Celem artykułu jest przedstawienie rozkładu współczynnika absorpcji SAR w ciele kobiety oraz szczegółowa analiza SAR w gruczołku piersiowym. Analizowane modele gruczołu piersiowego zostały podzielone na cztery kategorie na podstawie radiologicznej gęstości ich utkania. Symulacje numeryczne przeprowadzono za pomocą oprogramowania Empire XCcel opartego na metodzie różnic skończonych w dziedzinie czasu. Uzyskane wyniki porównano z obowiązującą dyrektywą (Dyrektywa 2013/35/UE). Wykazano, że tomografia mikrofalowa jest metodą bezpieczną.

Słowa kluczowe:

nowotwór gruczołu piersiowego, SAR (współczynnik absorpcji), pole elektromagnetyczne (PEM), tomografia mikrofalowa

Introduction

The high frequency electromagnetic field (PEM) impact on biological tissues is being investigated at numerous scientific centers around the world. Until now, precise and unambiguous standards of electromagnetic interactions on living organisms have not been precisely corrected, despite the recognition of their mechatronics. The long-term effects of electromagnetic fields on living organisms have not been recognized, which justifies the need to set up appropriate protection norms (Directive 2013/35/EU) [1,8].

One of the studied aspects of the problem is the attempt to introduce into the normative systems the value describing the energy processes in biological tissue under the influence of the electro-magnetic field. This value was named SAR (Specific Absorption Rate). Electromagnetic field interference can cause undesirable biological effects and, as a consequence, undesirable health effects (either temporary or permanent) [7].

Simultaneously with the research on harmfulness of PEMs for flora, fauna and humans, intensive research is conducted on the possibility of using them for the good of man. Biomedical studies that have been carried out to date have analyzed the good-to-life effects of PEM on the biosphere in a general way and on a human in more detail.

The electromagnetic field is used in a number of therapeutic therapies, including cancer, burns, cardiovascular diseases, arthritis and muscle disorders. The world is constantly looking for new methods to support basic diagnostic methods in medicine. Due to the frequent occurrence of breast cancer among women and the effectiveness of

appropriate early treatment, diagnostic methods are particularly important for the early detection of small tumors [3,5].

Numerical dosimetry, in comparison to experimental research, makes it possible to perform computer simulations quickly and easily. The disadvantage of this method is mainly the constraint associated with computer resources (memory, disk capacity).

In numerical doctrine, different phantom models are used from simple ones in homogeneous form to the most complex millimeter-sized structures. Unfortunately, the more complex an object is, the higher the hardware requirements of the computer on which the simulations are performed.

Microwave imaging involves the electromagnetic wave imaging of the object (breast) followed by measurement of the PEM spread or transmitted and the construction of the image on this basis [5,6].

Specyfic Absorption Rate

SAR can be defined as the time derivative of the energy entering the object with respect to its mass:

$$SAR(x, y, z) = \frac{1}{\rho} \cdot \frac{\partial W_c}{\partial t} \quad (1)$$

where: W_c – the energy entering the object Energy absorbed by the tissue in a unit of volume - J/m^3 , ρ – material density (tissue) – kg/m^3 .

In the scope of radio and microwave frequencies, the value of the absorption coefficient calculated locally depends on the square of the effective electric field E in the selected area of the human body. You can express it with a pattern:

$$SAR(x, y, z) = \sigma \frac{E^2}{\rho} \quad (2)$$

where: σ – conductivity of the material (tissue) – S/m.

The SAR value can also be determined on the basis of indirect effects of electromagnetic radiation, e.g., the increase in tissue temperature:

$$SAR(x, y, z) = C \frac{\delta T}{\delta t_E} \quad (3)$$

where: C – proper heat of material – $J \text{ kg}^{-1} \text{ K}^{-1}$, δT – temperature increase – K, δt_E – exposure time – s.

On the other hand, the mean SAR value in the whole or selected body area describes the total amount of power absorbed by the body (mass M):

$$SAR_{sred} = \frac{\iiint_V P_V \, dV}{M} \quad (4)$$

where: P_V – spatial distribution of the volume of absorbed power density in the body - W/m^3 , V – body volume – m^3 [7].

The normalized SAR is defined as the absorption capacity of the body normally or the small volume of the sample (usually 1 g or 10 g tissue). The safety guidelines for reducing exposure to electromagnetic fields have been published by the International Commission on Non-Ionizing Radiation Protection (IC-NIRP) [11]. In most countries, these guidelines have been adopted as basic SAR limits to prevent adverse effects on whole body health and excessive local tissue heating at frequencies from 100 kHz to 6 GHz. It

is important to specify the nature of the averaging in the SAR recommendations.

According to the recommendations of the Directive 2013/35/EU the level of influence (GPO) is presented in the table 1 [1].

Limit Impact Levels (GPOs) are values defined on the basis of biophysical and biological considerations, in particular supported by well-established scientific evidence of immediate and acute direct effects, i.e. thermal effects and electrical elimination of tissues. Top GPOs (GPOg) mean those GPOs beyond which employees may experience adverse health effects such as tissue warming or nervous and muscle tissue irritation. Lower GPOs (GPOd) mean those GPOs beyond which workers may experience temporary disturbances of sensory perception and minor changes in brain function [1]. Analyzing distribution of PEM and SAR are the fundation to estimates of exposure electromagnetic rate.

Numerical model of woman

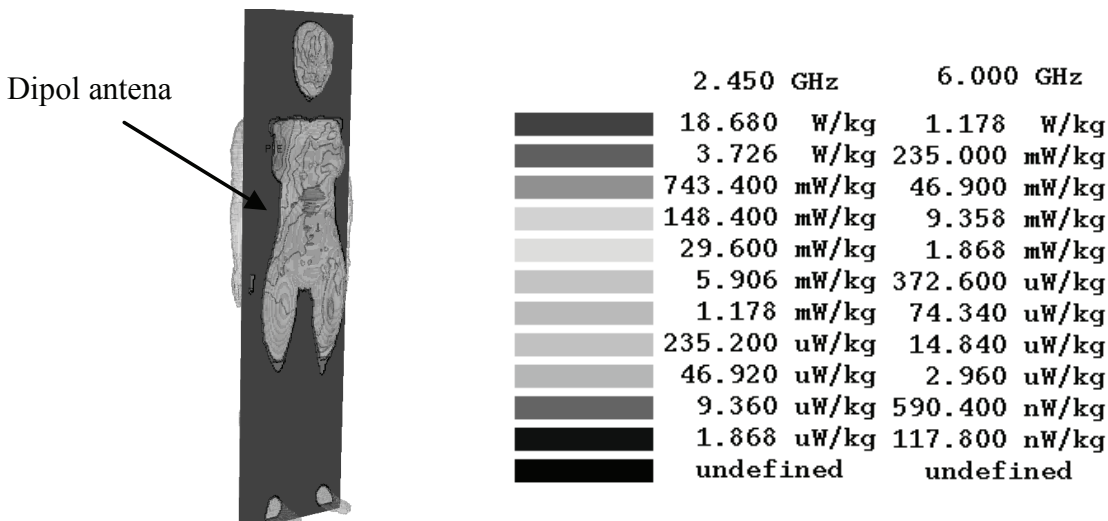
One of the basic tools used to evaluate the level of human exposure to electromagnetic fields is the numerical dosimetry, which enables the computer simulation of phenomena related to the absorption of electromagnetic energy by the human body.

For simulation one adopted the model of a 26-year-old woman weighing 58kg, from the ITIS Foundation [4]. Numerical analysis was performed using Empire XCcel software based on time-domain equations [5]. The model consists of 84 tissues with different electrical parameters (relative permeability, conductivity).

Table 1.

Top GPO values for exposure to electromagnetic fields in the frequency range 100 kHz to 6 GHz

GPOg	SAR values averaged over any six-minute period
GPO associated with total body heat stress expressed as SAR averaged in the body	0,4 W/kg
GPO related to local heat stress in the head and torso, expressed as local SAR in the body	10 W/kg
GPO associated with local heat stress in the limbs expressed as a local SAR in the body	20 W/kg

**Fig. 1**

Whole body of SAR at 2.45 GHz and 6 GHz frequencies

The essential property to be included in numerical simulations is the assumption of treatment of living matter as a real dielectric with frequency-dependent parameters. The most commonly used methods of dispersion of relative electrical permeability are Debye model and Cole Cole model [6]. For the needs of numerical simulations, the electrical parameters of biological tissues were calculated for frequencies of 2.45GHz and 6GHz based on the Debye equation. As a source of excitation, a 2.45 GHz and 6 GHz dipole transceiver (Tx/Rx) antenna was applied in the vicinity of the mammary gland in place of the most common tumor site in the gland. [4] Empire XCcel has adopted a dipole antenna model with a resistance of $R = 50 \Omega$. The dimensions of the antenna vary depending on the selected frequency. Antenna was shifted away from the model of the breast gland by $\lambda/2$, where – the wave length at the center.

First calculations were made for female models at 2.45 GHz.

Based on the analysis illustrated in Fig. 1 (for $f = 2,45$ GHz) absorption coefficient values were obtained $SAR_{AVR10g} = 77,66 \mu\text{W}/\text{kg}$, $SAR_{Max} = 18,68 \text{ W}/\text{kg}$. The simulation process was then performed for a frequency of 6 GHz. By analogy, the following values were obtained $SAR_{AVR10g} = 34,36 \mu\text{W}/\text{kg}$, $SAR_{Max} = 1,78 \text{ W}/\text{kg}$ for higher frequency 6 GHz).

Subsequently, a numerical analysis of the SAR was conducted in the context of the real mammary gland model. Analyzed breast gland was divided into four classes based on radiological density of the group

based on international ACR classification (American Collegeum of Radiologists) [10]:

- I – almost completely oily,
- II – dispersed adenoma-fibrous,
- III – with differentiated density,
- IV – very dense.

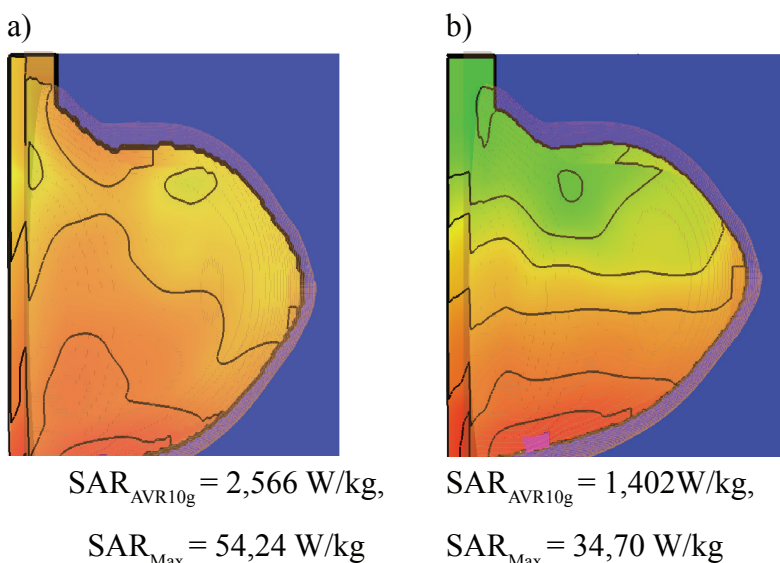
Database of images used for numerical breast models creation is located in research resources of the University of Wisconsin [4].

Absorption coefficients were obtained for different models of breast without and with modeling object of tumor with different electrical parameters (Fig. 2, 3, 4). Simulation was performed for two different transceiver antenna frequencies.

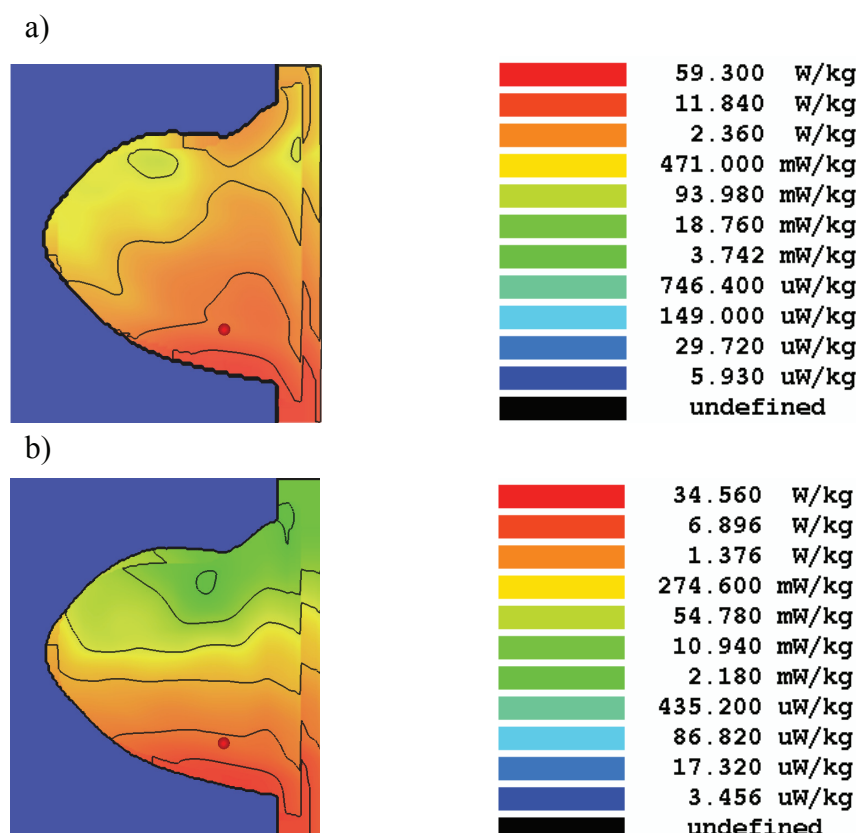
40 cases of breast cancer grade, tumor size (diameter 2, 6, 10, 22 mm) and frequency were analyzed. Some exemplary results of numerical simulation are presented in this paper.

The analyzed breast model of class I was constructed from 1832544 voxels ($nx = 101$, $ny = 112$, $nz = 162$) with a 5 mm eye edge. For the breast gland model of class I, one presented graphical distributions of SAR (Figure 2) for frequency $f = 2.45$ GHz and 6 GHz.

The average absorption coefficient obtained in Empire XCcel software is almost 2 times higher for 2.45 GHz compared to 6 GHz. The maximum value of the absorption coefficient is several times higher than the mean value (Figure 2). However, the area with the highest SAR value is located only at the location of the antenna. Figure 3 shows the SAR for class II breast gland with a tumor implant of 6 mm diameter.

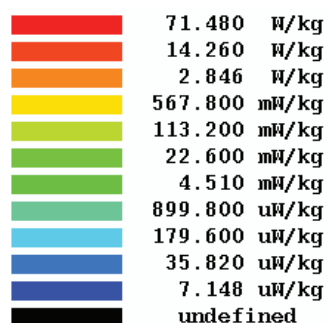
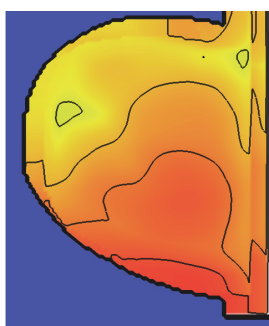
**Fig. 2**

SAR distribution in 3D realistic numerical breast Phantom class I with the space when the SAR value is maksimum, a) dla 2,45 GHz, b) 6 GHz

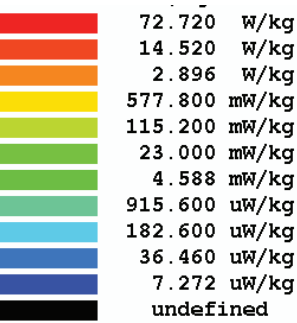
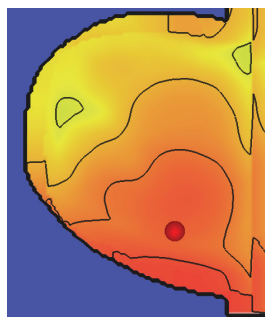
**Fig. 3.**

SAR value distribution of realistic numerical breast phantoms class II with tumor of diameter 6 mm, a) f = 2,45 GHz, SAR_{AVR10g} = 2,532 W/kg, b) f = 6 GHz, SAR_{AVR10g} = 1,396 W/kg

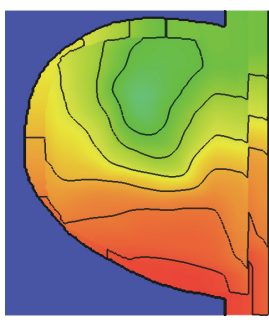
a)



b)



c)



d)

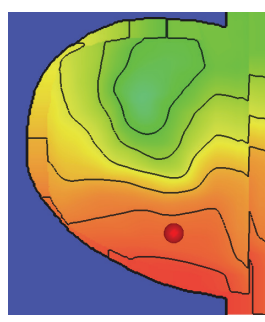
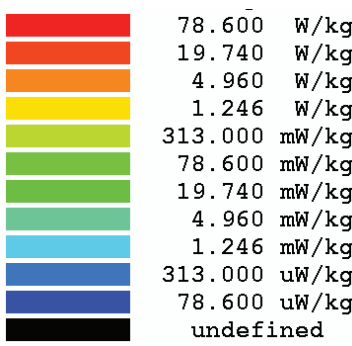
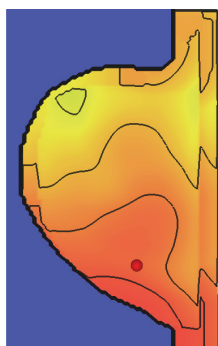


Fig. 4.

SAR value distribution of class III realistic numerical breast phantoms: a) $f = 2.45$ GHz, b) with tumor of diameter 10 mm, $f = 2.45$ GHz, c) $f = 6$ GHz, d) with tumor of diameter 10 mm, $f = 6$ GHz

a)



b)

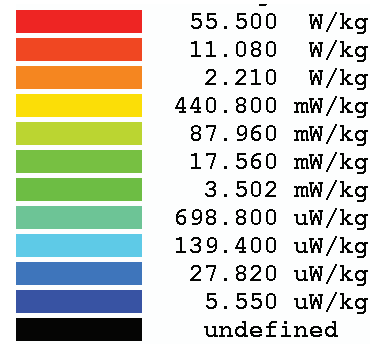
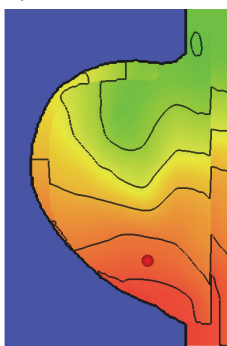
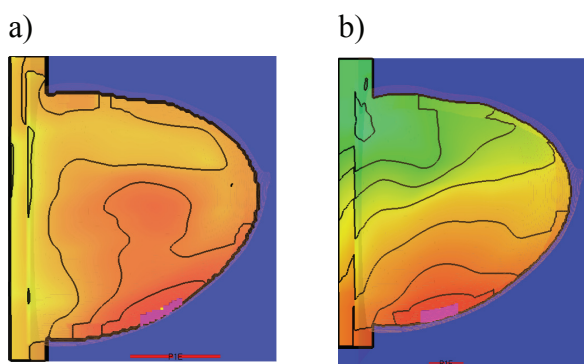


Fig. 5

SAR value distribution of realistic numerical breast phantoms: a) $f = 2.45$ GHz, with tumor of diameter 6 mm, b) $f = 6$ GHz with tumor of diameter 6 mm



$SAR_{AVR10g} = 2,554 \text{ W/kg}$, $SAR_{AVR10g} = 970 \text{ mW/kg}$,

$SAR_{Max} = 56,16 \text{ W/kg}$ $SAR_{Max} = 37,62 \text{ W/kg}$

Fig. 6.

SAR value distribution of realistic numerical breast phantoms class I when moving dipol antenna for frequencies, a) 2.45 GHz, b) 6 GHz

Figure 4 shows the differentiated density of the ACR breast gland.

The breast model of Class IV is shown in Figure 5.

On the basis of analysis for frequency of $f = 6 \text{ GHz}$ $SAR_{AVR10g} = 1,534 \text{ mW/kg}$ values were obtained for the model with a spherical object in place $SAR_{AVR10g} = 1,1544 \text{ mW/kg}$. For the models of breast gland of class IV, the average absorption coefficient is more than 2.5 times greater for the frequency of 2.45 GHz (fig. 5) than for 6 GHz.

When the antenna is moved to another location, the maximum absorption coefficient location is changed (fig. 6).

Analysis of all cases confirmed that the mean value of absorption coefficient is not very changed for models with spherical object and without objects. On the obtained images of the SAR distribution, it can be seen that the distributions are not homogeneous.

Conclusion

SAR analysis in the context of EM exposure has shown that this method makes it possible to evaluate and predict electromagnetic exposure of living organisms. It has been shown that the 6 GHz frequency is less invasive when determining the absorption coefficient. It should be emphasized that the absorption

coefficient in 3D models is lower when using a 6 GHz dipole antenna. On the other hand, the use of the 2.45 GHz frequency in spite of the higher absorption coefficient values obtained is in line with the standards laid down in the Directive (2013/35/EU).

Based on the obtained values of the absorption coefficient both in the context of the whole female body and of the composite models of the thoracic glands, it can be stated that the microwave radiation is safe in terms of electromagnetic exposure [7,9]. The cases analyzed did not exceed the maximum values given in the current Directive. The resulting SAR values are significantly lower than the limit values given in the current directive. Numerical simulations have confirmed that the area in which the maximum SAR value is determined depends on the location of the antenna.

Due to the difficulties in direct SAR measurement, it is very popular to use numerical dosimetry to determine SAR on the basis of knowledge of tissue parameters.

Based on a thorough analysis of the absorption coefficient, it can be said that microwave tomography is a safe method for the human body.

The use of microwave tomography for the detection of breast cancer as a method of supporting medical diagnostics certainly deserves consideration for continuing research in this field.

References

1. Dyrektywa 2013/35/UE Parlamentu Europejskiego i Rady z dnia 26 czerwca 2013 r. w sprawie minimalnych wymagań w zakresie ochrony zdrowia i bezpieczeństwa dotyczących narażenia pracowników na zagrożenia spowodowane czynnikami fizycznymi (polami elektromagnetycznymi) (dwudziesta dyrektywa szczegółowa w rozumieniu art. 16 ust. 1 dyrektywy 89/391/EWG) i uchylająca dyrektywę 2004/40/WE.
2. Gas P. Temperature inside tumor as time function in RF hyperthermia, Przegląd Elektrotechniczny 2010; 12.
3. Gas P. Tissue Temperature Distributions for Different Frequencies derived from Interstitial Microwave Hyperthermia, Przegląd Elektrotechniczny 2012; 12b.
4. <http://uwcem.ece.wisc.edu/phantomRepository.html#3d>,
5. Kurgan E., Gas P., Comparison of Polish and European Union Legislation On Protection Against Non-Ionizing Electromagnetic Fields. Poznan University of Technology Academic Journals, No 60 Electrical Engineering 2009.
6. Miaskowski A., Krawczyk A., Wac-Włodarczyk A. Zastosowanie promieniowania mikrofalowego w detekcji raka gruczołu piersiowego. Warszawa, CIOP-PIB 2007.
7. Miaskowski A. Zastosowanie mikrofal do detekcji raka sutka. Przegląd Elektrotechniczny 2005; 12.
8. Mika D., Michałowska J. Normatywne pomiary czynników szkodliwych na stanowisku pracy operatora obrabiarek sterowanych numerycznie. Przegląd Elektrotechniczny 2016; 12.
9. PN-T-06580:2002 Ochrona pracy w polach i promieniowaniu elektromagnetycznym w zakresie częstotliwości od 0 Hz do 300 GHz. Arkusz 01. Terminologia. Arkusz 03. Metody pomiaru i oceny pola na stanowisku pracy.
10. Zastrow E., Davis S.K., Lazebnik M., Kelcz F., Van Veen B.D., and Hagness S.C. Development of anatomically realistic numerical breast phantoms with accurate dielectric properties for modeling microwave interactions with the human breast. *IEEE Transactions on Biomedical Engineering* 2008; 55(12): 2792-2800.
11. Zhang M., Alden A. Calculation of Whole-Body SAR from a 100 MHz Dipole Antenna. *Progress In Electromagnetics Research* 2011; 119: 133-153.